Scientific Research Publishing

Journal of Applied Mathematics and Physics, 2025, 13(9), 3163-3172
https://www.scirp.org/journal/jamp
ISSN Online: 2327-4379
ISSN Print: 2327-4352

Angular Distribution Effect on Bremsstrahlung Radiation Produced by Boron and Aluminum

Ratibah Jaber Almatrafi, Sadah Abdullah Alkhateeb, Nada Ahmed Almuallem

Department of Mathematics and Statistics, University of Jeddah, Jeddah, Saudi Arabia
Email: RALMATRAFI.stu@uj.edu.sa, salkhateeb@uj.edu.sa, naalmouallim@uj.edu.sa

How to cite this paper: Almatrafi, R.J., Alkhateeb, S.A. and Almuallem, N.A. (2025) Angular Distribution Effect on Bremsstrahlung Radiation Produced by Boron and Aluminum. *Journal of Applied Mathematics and Physics*, **13**, 3163-3172.
https://doi.org/10.4236/jamp.2025.139179

Received: August 16, 2025
Accepted: September 23, 2025
Published: September 26, 2025

Abstract

This study calculates the angular distribution of Bremsstrahlung radiation for B_{11}^{5} and Al_{27}^{13} according to the Bethe-Heitler equation. We compare the electromagnetic effects of radiation emitted by photons colliding with Aluminum and Boron nuclei, applying the mathematical program "Mathematica". We compare the impact of magnetic and electric cross-sections on Bremsstrahlung radiation production. We will use graphs to study the effect of electric and magnetic fields on Bremsstrahlung radiation creation. In addition, we examine how atomic mass affects Bremsstrahlung radiation emission. According to our results, magnetic interactions can be used to produce X-rays with specific properties.

Keywords

Bremsstrahlung Radiation, Bethe-Heitler Equation, Angular Distribution, Cross Section

1. Introduction

The angular distributions of photons in Bremsstrahlung radiation between electrons and atoms are of wide-ranging practical importance [1]. Information on Bremsstrahlung radiation's angular distribution is essential in many fields. It is crucial for improving imaging techniques in medical and industrial applications which ensures accurate diagnosis and analysis. For example, radiation physics, nuclear physics, radiotherapy, astrophysics, plasma physics, and fusion [2]. In 1966, measurements of photon angular distributions for fixed directions of the emission of electrons [3]-[5] were published. The experiments used a 300 keV electron energy, with a gold foil as the target. A selection was made of outgoing electrons with an energy of 170 keV and scattering angles of 0˚, 5˚, and 10˚. Since the experimental

values were only relative, they were calculated with respect to the Elwert and Haug theoretical curves at the maximum of their angular distributions [6]. In [7], initial measurements of the absolute cross-section at one point within the angular distribution showed that gold's cross-section is underestimated by the calculation, while in [8] an excellent agreement was found for aluminium ($Z=13$). Aehlig and Scheer discussed an angular distribution of the absolute triple differential cross-section of silver targets ($Z=47$) [9]. In addition, experimental cross-sections were compared with results from Elwert and Haug's form-factor screening. The partial-wave results of Keller and Dreizler are presented in [10]. Many experiments have used 50 keV incident electrons and two targets, Al and Au, with photon emission angles ranging from 10˚ to 180˚ [11]-[13]. Furthermore, the studies [14] and [15] included multiple targets between C and U, emission angles of 90˚, and incident electron energies of 75 and 100 keV. In 2011, a study by Gonzales, Cavness, and Williams [16] concentrated on the angular distribution of Bremsstrahlung caused by electrons incident on a thick Ag target with initial energies ranging from 10 to 20 keV. Bhupendra Singh, Suman Prajapati, *et al.* [15] measured the angular distribution of Bremsstrahlung photons produced by 10 - 25 keV electrons incident on Ti and Cu targets [2].

Previous studies on Bremsstrahlung radiation looked at high-energy electrons (100 keV to several GeV) hitting heavy atoms like gold ($Z=79$) and silver ($Z=47$) For example, Nakel's experiments (1966-1968) measured how photons spread at 300 keV using gold [3]-[5], and other works checked radiation strength for Aluminum ($Z=13$) and silver [7]-[9]. Our study uses very high energies (300 - 800 GeV) with lighter atoms (Boron, $Z=5$; Aluminum, $Z=13$ to learn more about how magnetic effects create radiation.

The Bethe-Heitler equation, used to model Bremsstrahlung, assumes a simple nucleus and ignores effects like Coulomb corrections, which can make radiation calculations less accurate at 300 - 800 GeV, especially for an Aluminum $Z=13$ [17] [18]. Our study looks at how magnetic effects work with lighter atoms (Boron and Aluminum) at very high energies, helping improve knowledge of particle accelerators and space science [19].

In our paper, we study the angular distributions of Bremsstrahlung radiation emitted from Aluminum ($Z=13$) and Boron ($Z=5$) atoms with incident electron energies of 300 GeV, 600 GeV, and 800 GeV. The incident angles θ varied between 60˚ and 180˚. The structure of this paper is as follows: In Section 2, we describe the methodology used to study the angular distribution of Bremsstrahlung radiation, including the application of the Bethe-Heitler equation and the decomposition of the cross-section into electric and magnetic components. Section 3 presents the main results, including the effect of electric and magnetic cross sections on both Boron and Aluminum atoms, along with a comparison based on atomic number. Finally, in Section 4, we summarize our findings and discuss their implications in the context of X-ray generation and high-energy radiation analysis.

2. Methodology

In this section, we present the theoretical framework and methodology used in our analysis, including the simplification of the Bethe-Heitler equation and its decomposition into electric and magnetic equations. Bremsstrahlung radiation will be given off by Aluminum and Boron atoms when electrons hit them with energies between 300 and 800 GeV and at angles between 60˚ and 180˚ degrees. We study the angular distributions of the Bremsstrahlung radiation emitted. Equation (1) shows the Bethe-Heitler differential cross-section for Bremsstrahlung radiation. The formula describes the energy of the radiation emitted when the electric field causes the electron to slow down. It is studied at high energies and different angles of incidence [17].

$$\begin{aligned} \mathrm{d}\sigma = & \frac{Z^2\alpha^3}{(2\pi)^2}\frac{|p|}{|p_0|}\frac{\mathrm{d}\omega}{\omega}\frac{\mathrm{d}\Omega_0\mathrm{d}\Omega}{|q|^4}\frac{p_0^2\sin^2\theta_0}{(E_0-p_0\cos\theta_0)^2}\left(4E^2-q^2\right) \\ & +\frac{p^2\sin^2\theta}{(E-P\cos\theta)^2}\left(4E_0^2-q^2\right)+2\omega^2\frac{p^2\sin^2\theta+p_0^2\sin^2\theta_0}{(E-p\cos\theta)(E_0-p_0\cos\theta_0)} \\ & -2\frac{p_0p\sin\theta\sin\theta_0\cos\varphi}{(E-p\cos\theta)(E_0-P_0\cos\theta_0)}\left(2E^2+2E_0^2-q^2\right) \end{aligned} \tag{1}$$

Equation (1) represents the Bethe-Heitler formula for Bremsstrahlung radiation, each symbol has a specific meaning related to the scattering process and the properties of the photon and electron, as follows:

$\mathrm{d}\sigma$: Differential cross-section. It quantifies the likelihood of radiation being emitted into a specific solid angle $\mathrm{d}\Omega_0$ and $\mathrm{d}\Omega$.

Z: The atomic number of the target nucleus, for Boron nuclei ($Z=5$) and for Aluminum ($Z=13$)

α: The fine-structure constant, $\alpha \approx 1/137$. representing the strength of the electromagnetic interaction.

π: The mathematical constant $\pi \approx 3.14159$

p_0, p: The initial and final momenta of the electron before and after the emission of the Bremsstrahlung photon.

ω: The energy of the emitted Bremsstrahlung photon.

E_0, E: The initial and final energies of the electron before and after photon emission, respectively.

q: The momentum transfer between the electron and the nucleus, $q = p_0 - p$. This represents the difference between initial and final momenta of the electron.

θ_0: The angle of the emitted photon relative to the initial direction of the electron's momentum.

θ: The scattering angle of the final electron, *i.e.*, the angle between the final momentum of the electron p and its initial momentum.

φ: The azimuthal angle between the planes of the initial and final electron directions, influencing how the scattering occurs in 3D space.

$\mathrm{d}\Omega_0$: The solid angle of the emitted photon.

$\mathrm{d}\Omega$: The solid angle of the scattered electron.

$d\omega$: The energy differential, typically indicating a small change in the electron's energy during the process.

The simplified Bethe-Heitler Equation (2) separates radiation into electric and magnetic parts, as shown in [20]. The original Bethe-Heitler equation Equation (1) calculates total radiation but doesn't split it into electric or magnetic parts. Based on [20] [21], Equation (2) is written as:

$$d\sigma = d\sigma_{EC} + d\sigma_{MD} + d\sigma_{EQ} + d\sigma_{MO} \tag{2}$$

The $d\sigma_{EC}, d\sigma_{MD}, d\sigma_{EQ}$ and $d\sigma_{MO}$ are Electric Charge (EC), Magnetic Dipole (MD), Electric Quadrupole (EQ), and Magnetic Octupole (MO) respectively. where,

$$d\sigma_{EC} = 8\times\pi\times\zeta\times\phi_{EC} \tag{3}$$

$$d\sigma_{MD} = 8\times\pi\times\zeta\times\left(\frac{\mu_1}{z\times e}\right)^2\times a_{MD}\times\phi_{MD} \tag{4}$$

$$d\sigma_{EQ} = 8\times\pi\times\zeta\times\left(\frac{Q}{z\times e}\right)^2\times a_{EQ}\times\phi_{EQ} \tag{5}$$

$$d\sigma_{MO} = 8\times\pi\times\zeta\times\left(\frac{\Omega}{z\times e}\right)^2\times a_{MO}\times\phi_{MO} \tag{6}$$

and,

$$\zeta = \frac{z^2\alpha^3}{4\pi^2}\cdot\frac{k^+}{k^-\chi} \tag{7}$$

$$a_{MD} = \frac{s+1}{3s}, a_{EQ} = \frac{(s+1)\cdot(2s+3)}{180s\cdot(2s-1)}, a_{MO} = \frac{2\cdot(s+1)\cdot(s+2)\cdot(2s+3)}{4725s\cdot(s-1)\cdot(2s-1)} \tag{8}$$

where (MD), (EQ), and (MO) are coefficients of the nucleus with spin s, ($s=1.5$ for the Boron atom and $s=2.5$ for the Aluminum atom).

The Bremsstrahlung photons γ are produced in electron interaction with the nuclear field [22].

We can represent the interaction equation as:

$$e_i^- + N \to N + e_f^- + \gamma \tag{9}$$

The Feynman diagrams for this process are shown in **Figure 1**.

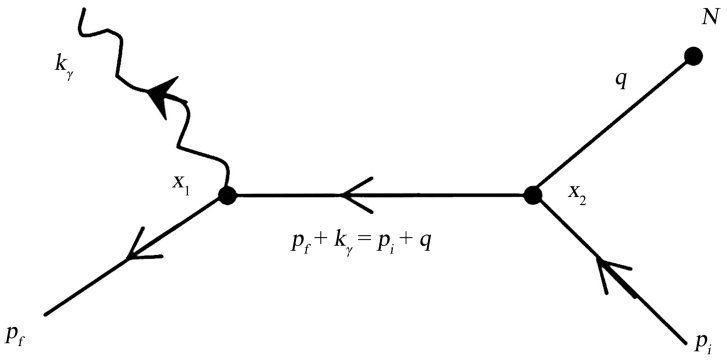

(a)

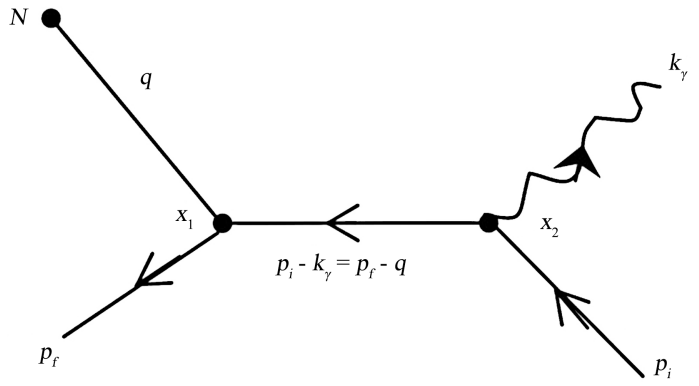

(b)

Figure 1. Feynman diagrams for Bremsstrahlung processes.

There are two cases in which the Bremsstrahlung process can occur: case (a): the electron enters with momentum p_i, interacts with the Coulomb field N of the atom and consequently produces a scattered electron with momentum p_f, and a scattered photon with momentum k_γ. Or case (b): the incident electron with momentum p_i collides with the Coulomb field N of the atom, first emits a photon with momentum, k_γ and then produces a scattered electron with momentum p_f [18] [23].

We chose the 300 - 800 GeV energy range to study high-energy Bremsstrahlung radiation, which is important for particle accelerators and space science. Boron ($Z=5$) and Aluminum ($Z=13$) are light atoms. Our study compares their radiation to understand their differences.

3. Main Results

We studied the impact of the electric and magnetic cross sections of boron and aluminum atoms on the production of Bremsstrahlung radiation. The $\mathrm{d}\sigma_{\mathrm{E1}}$ and $\mathrm{d}\sigma_{\mathrm{M1}}$ represent the electric and magnetic cross sections for Boron, respectively, while $\mathrm{d}\sigma_{\mathrm{E2}}$ and $\mathrm{d}\sigma_{\mathrm{M2}}$ represent the electric and magnetic cross sections for Aluminum, respectively.

3.1. Effect of Electric and Magnetic Cross-Sections on the Boron Atom

- The electrical cross sections of Boron nuclei decrease with increasing energy and angle of incidence, as shown in **Figure 2**. For example:

$$\mathrm{d}\sigma_{\mathrm{E1}} = 2.58442\times10^{-34} \quad \text{at } \epsilon = 300 \text{ GeV and } \theta = 100^{\circ},$$
$$\mathrm{d}\sigma_{\mathrm{E1}} = 3.40419\times10^{-35} \quad \text{at } \epsilon = 300 \text{ GeV and } \theta = 150^{\circ}.$$

- The magnetic cross-sections of Boron nuclei increase as both the energy and incident angle increase, as shown in **Figure 3**. For example:

$$\mathrm{d}\sigma_{\mathrm{M1}} = 3.2649\times10^{-20} \quad \text{at } \epsilon = 800 \text{ GeV and } \theta = 80^{\circ},$$
$$\mathrm{d}\sigma_{\mathrm{M1}} = 1.04118\times10^{-19} \quad \text{at } \epsilon = 800 \text{ GeV and } \theta = 160^{\circ}.$$

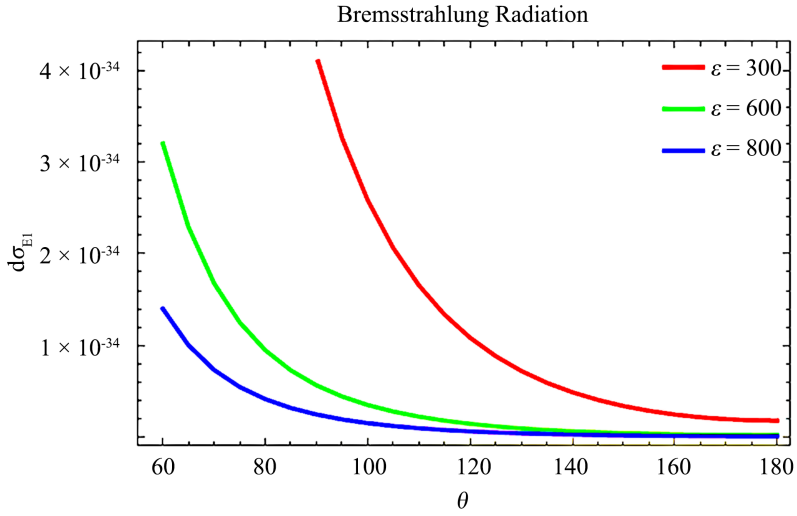

Note that $d\sigma_{E1}$ is more effective at energy $\epsilon = 300$ GeV and angle $\theta = 60^{\circ}$.

Figure 2. Electric cross-sections for B_{11}^{5} atom at $\epsilon = 300, 600, 800$ GeV.

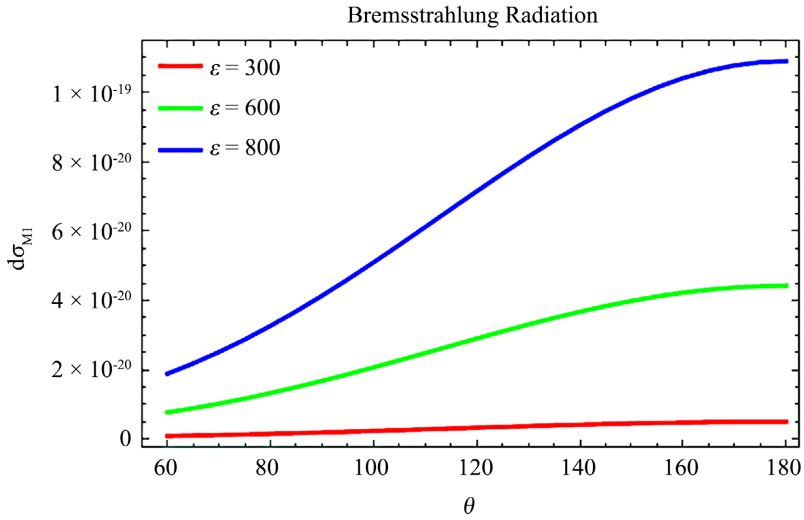

Note that $d\sigma_{M1}$ is more effective at energy $\epsilon = 800$ GeV and angle $\theta = 180^{\circ}$.

Figure 3. Magnetic cross-sections for B_{11}^{5} atom at $\epsilon = 300, 600, 800$ GeV.

3.2. Effect of Electric and Magnetic Cross-Sections on the Aluminum Atom

- The electric cross-sections for Aluminum nuclei decrease as both the energy and incident angle increase, as shown in **Figure 4**. For example:

$$d\sigma_{E2} = 6.41969 \times 10^{-34} \quad \text{at } \epsilon = 600 \text{ GeV and } \theta = 80^{\circ},$$
$$d\sigma_{E2} = 4.42364 \times 10^{-35} \quad \text{at } \epsilon = 600 \text{ GeV and } \theta = 140^{\circ}.$$

- The magnetic cross-sections of Aluminum nuclei increase as both the energy and incident angle increase, as shown in **Figure 5**. For example:

$$d\sigma_{M2} = 4.83087 \times 10^{-21} \quad \text{at } \epsilon = 800 \text{ GeV and } \theta = 80^{\circ},$$
$$d\sigma_{M2} = 1.59491 \times 10^{-20} \quad \text{at } \epsilon = 800 \text{ GeV and } \theta = 170^{\circ}.$$

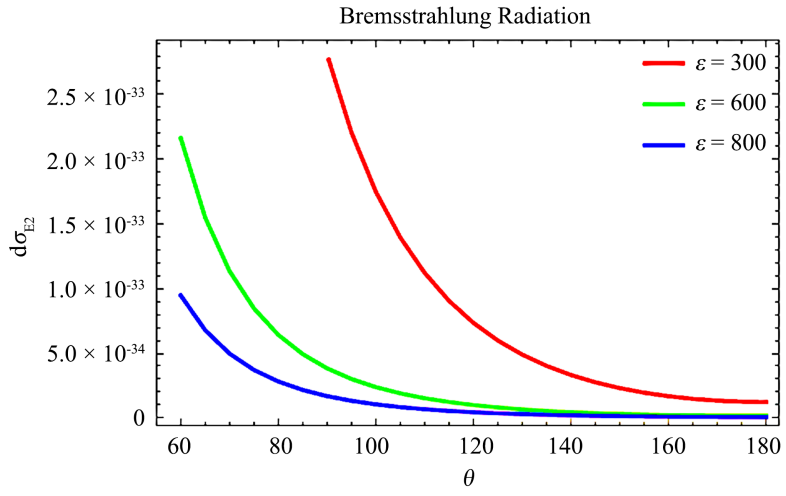

Note that $d\sigma_{E2}$ is more effective at energy $\epsilon = 300\,\text{GeV}$ and angle $\theta = 60^{\circ}$.

Figure 4. Electric cross-sections for Al_{27}^{13} atom at $\epsilon = 300, 600, 800\,\text{GeV}$.

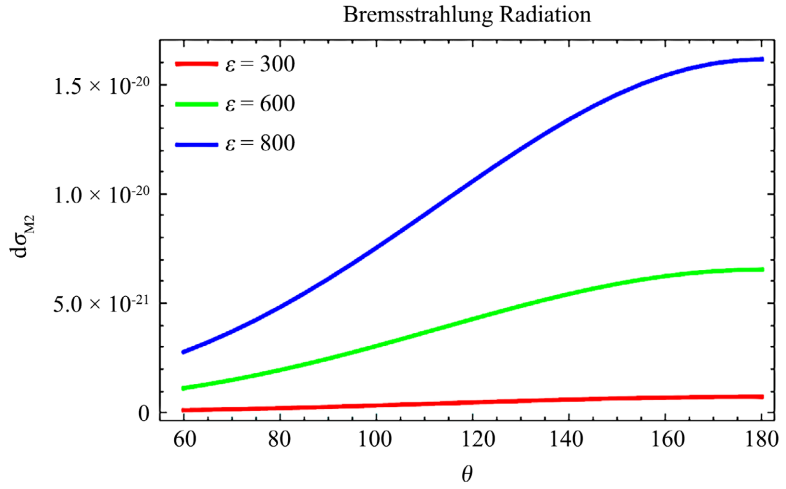

Note that $d\sigma_{M2}$ is more effective at energy $\epsilon = 800\,\text{GeV}$ and angle $\theta = 180^{\circ}$.

Figure 5. Magnetic cross-sections for Al_{27}^{13} atom at $\epsilon = 300, 600, 800\,\text{GeV}$.

3.3. Effect of Atomic Number

- The electrical cross sections of the Aluminum atom are more effective in producing Bremsstrahlung radiation than the electrical cross sections of the Boron atom, as shown in **Figure 6**. For example:

$$d\sigma_{E1} = 4.90264 \times 10^{-35} \quad \text{at } \theta = 140^{\circ},$$
$$d\sigma_{E2} = 3.31484 \times 10^{-34} \quad \text{at } \theta = 140^{\circ}.$$

- The magnetic cross sections of the Boron atom are more effective in producing Bremsstrahlung radiation than the magnetic cross-sections for the Aluminum atom, as shown in **Figure 7**. For example:

$$d\sigma_{M1} = 3.27241 \times 10^{-21} \quad \text{at } \theta = 120^{\circ},$$
$$d\sigma_{M2} = 4.84199 \times 10^{-22} \quad \text{at } \theta = 120^{\circ}.$$

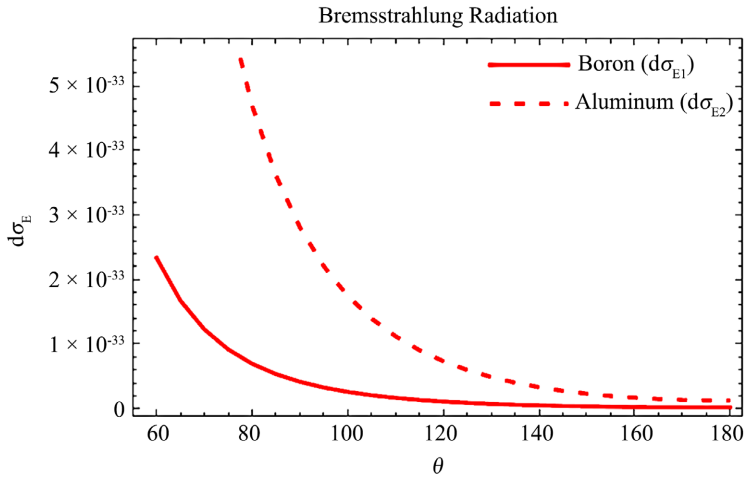

Note that the electric cross-sections of the higher-mass Aluminum ($Z=13$) are more effective in producing Bremsstrahlung radiation than those of the lighter-mass Boron ($Z=5$).

Figure 6. Comparison of electric cross-sections of B_{11}^{5}, Al_{27}^{13} at $\epsilon = 300\ \text{GeV}$.

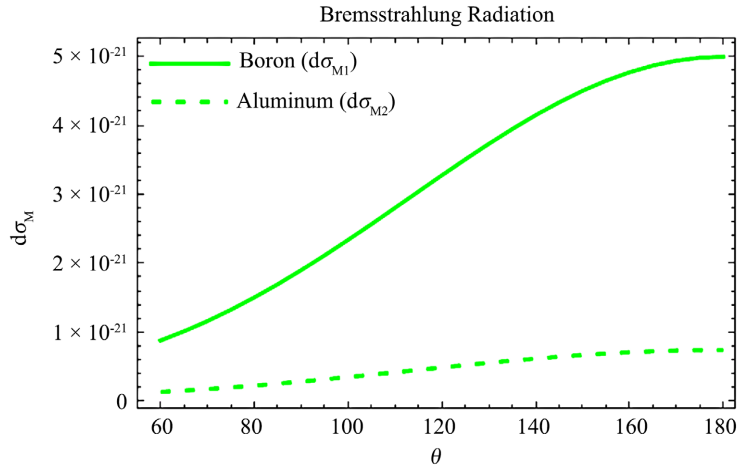

Note that the magnetic cross-sections of lighter mass Boron ($Z=5$) are more effective in producing Bremsstrahlung radiation than those of the higher mass Aluminum ($Z=13$).

Figure 7. Comparison of magnetic cross-sections of B_{11}^{5}, Al_{27}^{13} at $\epsilon = 300\ \text{GeV}$.

4. Conclusion

Our results show that at high energies (300 - 800 GeV), magnetic cross sections of Boron ($Z=5$) and Aluminum ($Z=13$) play an important role in producing Bremsstrahlung radiation, while electric cross sections are less important. Specifically, Aluminum has stronger electric cross sections than Boron, whereas Boron has stronger magnetic cross sections. These findings show the importance of magnetic interactions at high energies [24] and can help in designing special X-ray sources or experiments that increase magnetic effects. Although typical X-ray sources work at lower energies (keV-MeV) where electric interactions dominate [2], this provides useful ideas for future high-energy applications.

Conflicts of Interest

The authors declare no conflicts of interest regarding the publication of this paper.

References

[1] García-Alvarez, J.A., Fernández-Varea, J.M., Vanin, V.R. and Maidana, N.L. (2018) Electron-Atom Bremsstrahlung Cross Sections in the 20-100 keV Energy Region: Absolute Measurements for 6 ≤ Z ≤ 79 and Comparison with Theoretical Databases. *Journal of Physics B*: *Atomic*, *Molecular and Optical Physics*, **51**, Article ID: 225003. https://doi.org/10.1088/1361-6455/aae6e8

[2] Singh, B., Prajapati, S., Kumar, S., Singh, B.K., Llovet, X. and Shanker, R. (2018) Measurement of the Angular Distribution of Thick Target Bremsstrahlung Produced by 10-25 keV Electrons Incident on Ti and Cu Targets. *Radiation Physics and Chemistry*, **150**, 82-89. https://doi.org/10.1016/j.radphyschem.2018.04.027

[3] Nakel, W. (1966) Koinzidenzexperimente am elementarprozess der bremsstrahlungserzeugung. *Physics Letters*, **22**, 614-615. https://doi.org/10.1016/0031-9163(66)90678-0

[4] Nakel, W. (1967) Zum elementarprozess der bremsstrahlungserzeugung. *Physics Letters A*, **25**, 569-570. https://doi.org/10.1016/0375-9601(67)90262-9

[5] Nakel, W. (1968) Koinzidenzexperimente zum Elementarprozeß der Bremsstrahlungserzeugung. *Zeitschrift für Physik A Hadrons and Nuclei*, **214**, 168-178. https://doi.org/10.1007/bf01379801

[6] Elwert, G. and Haug, E. (1969) Calculation of Bremsstrahlung Cross Sections with Sommerfeld-Maue Eigenfunctions. *Physical Review*, **183**, 90-105. https://doi.org/10.1103/physrev.183.90

[7] Kreuzer, K. and Nakel, W. (1971) Absolute Cross-Section Measurement of the Elementary Process of Bremsstrahlung Production for Gold at 300 keV. *Physics Letters A*, **34**, 407-408. https://doi.org/10.1016/0375-9601(71)90940-6

[8] Nakel, W. and Sailer, U. (1970) Absolute Cross Section Measurement of the Elementary Process of Bremsstrahlung Production. *Physics Letters A*, **31**, 181-182. https://doi.org/10.1016/0375-9601(70)90912-6

[9] Aehlig, A. and Scheer, M. (1972) Absolutmessungen des Elementarprozesses der Bremsstrahlungserzeugung. *Zeitschrift für Physik A Hadrons and nuclei*, **250**, 235-247. https://doi.org/10.1007/bf01387460

[10] Keller, S. and Dreizler, R.M. (1997) Relativistic Independent Particle Approximation Study of Triply Differential Cross Sections for Electron-Atom Bremsstrahlung. *Journal of Physics B*: *Atomic*, *Molecular and Optical Physics*, **30**, 3257-3266. https://doi.org/10.1088/0953-4075/30/14/016

[11] Shaffer, C.D., Tong, X. and Pratt, R.H. (1996) Triply Differential Cross Section and Polarization Correlations in Electron Bremsstrahlung Emission. *Physical Review A*, **53**, 4158-4163. https://doi.org/10.1103/physreva.53.4158

[12] Motz, J.W. and Placious, R.C. (1958) Bremsstrahlung Cross-Section Measurements for 50-keV Electrons. *Physical Review*, **109**, 235-242. https://doi.org/10.1103/physrev.109.235

[13] Rester, D.H., Edmonson, N. and Peasley, Q. (1970) Bremsstrahlung Cross Sections for Al and Au for Incident-Electron Energies of 0.05 and 0.20 Mev. *Physical Review A*, **2**, 2190-2196. https://doi.org/10.1103/physreva.2.2190

[14] Quarles, C.A. and Heroy, D.B. (1981) Atomic-Field Bremsstrahlung from 50-140 keV

Electrons. *Physical Review A*, **24**, 48-54. https://doi.org/10.1103/physreva.24.48

[15] Ambrose, R., Altman, J.C. and Quarles, C.A. (1987) Atomic-Field Bremsstrahlung Cross Sections for Incident Electron Energy from 50 to 100 keV for Atomic Numbers from 6 to 92. *Physical Review A*, **35**, 529-539. https://doi.org/10.1103/physreva.35.529

[16] Gonzales, D., Cavness, B. and Williams, S. (2011) Angular Distribution of Thick-Target Bremsstrahlung Produced by Electrons with Initial Energies Ranging from 10 to 20 keV Incident on Ag. *Physical Review A*, **84**, Article ID: 052726. https://doi.org/10.1103/physreva.84.052726

[17] Zhu, W. (2020) Improved Bethe-Heitler Formula. *Nuclear Physics B*, **953**, Article ID: 114958. https://doi.org/10.1016/j.nuclphysb.2020.114958

[18] Morgan, S.H. (1970) Coulomb Corrections to the Bethe-Heitler Cross Sections for Electron-Nucleus Bremsstrahlung. NASA Technical Report. https://ntrs.nasa.gov/citations/19710001524

[19] Haug, E. and Nakel, W. (2004) The Elementary Process of Bremsstrahlung. World Scientific Publishing. https://doi.org/10.1142/9789812795007

[20] Alkhateeb, S.A., Alshaery, A.A. and Aldosary, R.A. (2022) Electron-Positron Pair Production in Electro-Magnetic Field. *Journal of Applied Mathematics and Physics*, **10**, 237-244. https://doi.org/10.4236/jamp.2022.102017

[21] Alkhateeb, S.A., Alshaery, A.A. and Aldosary, R.A. (2022) Leptonic Pair Production in Electromagnetic Field. *Nuclear Science*, **7**, 34-38.

[22] Al-Khateeb, S. (2023) Polarization Dependence of the Bremsstrahlung Cross-Section in Atomic Systems. *Journal of Physics G: Nuclear and Particle Physics*, **50**, Article ID: 125101.

[23] Feynman, R.P. (2018) Quantum Electrodynamics. CRC Press.

[24] Almatrafi, R.J., Alkhateeb, S.A. and Almuallem, N.A. (2025) Energy Distribution Effect on Bremsstrahlung Radiation Produced by B_{11}^{5} and Al_{27}^{13}. *International Journal of Analysis and Applications*, **23**, 33. https://doi.org/10.28924/2291-8639-23-2025-33